STEM CELLS®
Original Article

Derivation and Characterization of New Human Embryonic Stem Cell Lines: SNUhES1, SNUhES2, and SNUhES3

SUN KYUNG OH,[a,b] HEE SUN KIM,[a,b] HEE JIN AHN,[b] HYE WON SEOL,[b] YOON YOUNG KIM,[b] YONG BIN PARK,[b] CHUL JONG YOON,[c] DONG-WOOK KIM,[d] SEOK HYUN KIM,[a,b] SHIN YONG MOON[a,b]

[a]Department of Obstetrics and Gynecology and [b]Institute of Reproductive Medicine and Population, Medical Research Center, College of Medicine, Seoul National University, Seoul, Korea; [c]Laboratory of Electron Microscope, Seoul National University Children's Hospital, Seoul, Korea; [d]Department of Physiology, Yonsei University College of Medicine, Seoul, Korea

Key Words. Cell replacement therapy • Derivation of hESCs • Differentiation into cardiomyocytes EM analysis of hESCs • Human embryonic stem cells

ABSTRACT

Here we report the derivation and characterization of new human embryonic stem cell (hESC) lines, SNUhES1, SNUhES2, and SNUhES3. These cells, established from the inner cell mass using an STO feeder layer, satisfy the criteria that characterize pluripotent hESCs: The cell lines express high levels of alkaline phosphatase, cell surface markers (such as SSEA-3, SSEA-4, TRA-1-60, and TRA-1-81), transcription factor Oct-4, and telomerase. When grafted into severe combined immunodeficient mice after prolonged proliferation, these cells maintained the developmental potentials to form derivatives of all three embryonic germ layers. The cell lines have normal karyotypes and distinct identities, revealed from DNA fingerprinting. Interestingly, analysis by electron microscopy clearly shows the morphological difference between undifferentiated and differentiated hESCs. Undifferentiated hESCs have a high ratio of nucleus to cytoplasm, prominent nucleoli, indistinct cell membranes, free ribosomes, and small mitochondria with a few crista, whereas differentiated cells retain irregular nuclear morphology, desmosomes, extensive cytoplasmic membranes, tonofilaments, and highly developed cellular organelles such as Golgi complex with secretory vesicles, endoplasmic reticulum studded with ribosomes, and large mitochondria. Existence of desmosomes and tonofilaments indicates that these cells differentiated into epithelial cells. When in vitro differentiation potentials of these cell lines into cardiomyocytes were examined, SNUhES3 was found to differentiate into cardiomyocytes most effectively.
STEM CELLS *2005;23:211–219*

INTRODUCTION

Since mouse embryonic stem cells (mESCs) were isolated and cultured in vitro two decades ago [1, 2], the research of ESCs has made outstanding contributions to our understanding of developmental biology. ESCs, derived from the inner cell mass (ICM) in preimplantation embryos, can proliferate extensively in vitro while maintaining an undifferentiated state and differentiate into most cell types under certain conditions [3–8]. This ability of ESCs makes them a good source for cell replacement therapy [9]. In addition, ESCs can be used

Correspondence: Shin Yong Moon, M.D., Ph.D., Department of Obstetrics and Gynecology, College of Medicine, Seoul National University, 28 Yongon-dong, Chongno-gu, Seoul 110-744, Korea. Telephone: 82-2-2072-2384; Fax: 82-2-3672-7601; e-mail: shmoon@plaza.snu.ac.kr; and Dong-Wook Kim, Ph.D., Yonsei University College of Medicine, Department of Physiology, 134 Shinchon-dong, Seodaemun-gu, Seoul 120-752, Korea. Telephone: 82-2-361-5208; Fax: 82-2-393-0203; e-mail: dwkim2@yumc.yonsei.ac.kr Received May 26, 2004; accepted for publication October 7, 2004. 1066-5099/2005/$12.00/0 doi: 10.1634/stemcells.2004-0122

as a source for study of basic developmental biology, identification of factors that are involved in regulation of developmental processes and differentiation into certain cells or tissue, and screening for drugs or toxins [4].

Human ESC (hESC) lines have been successfully derived from human blastocysts [10–13]. Derivation and characterization of hESCs is very important in terms of the direct application to human diseases. Like mESCs, the essential characteristics of hESCs include (a) derivation from the preimplantation embryos, (b) prolonged proliferation in vitro, and (c) stable developmental potentials to form derivatives of all three embryonic germ layers even after prolonged culture. However, hESCs are different from mESCs in the expression of markers. Stage-specific embryonic antigen-1 (SSEA-1), a cell surface marker, is expressed in mESCs but not in hESCs [10–13]. In contrast, SSEA-3, SSEA-4, TRA-1-60, and TRA-1-81 are markers that are expressed only in hESCs [10–13].

Recently, several studies have shown that neuronal cells [14–16], cardiomyocytes [3], and pancreatic β cells [17] can be induced from hESCs. These results give promise to the clinical application of hESCs for the treatment of diseases such as Parkinson's disease, diabetes, and heart disease. However, ESCs can display different differentiation potentials under the same conditions [18–21]. Thus, testing the differentiation potentials of existing ESC lines is critical in the selection of the appropriate cell line for each experimental purpose. For cell replacement therapy in the field of neurological disorders, the cell lines that most effectively give rise to neuronal populations will be useful. Accordingly, establishment and characterization of many hESC lines are important in this respect.

Here we report the establishment of new hESC lines, SNUhES1, 2, and 3. We observed that these cells have the same characteristics as the existing hESC lines in the undifferentiated state and can differentiate into cardiomyocyte lineage in vitro. In addition, our analysis by electron microscopy (EM) shows that the undifferentiated hESCs and differentiated cells are clearly different in their cellular structure.

Materials and Methods

Culture from Pronuclear Stage Human Embryo to Blastocyst

For derivation of hESC lines, cryopreserved pronuclear stage embryos were donated for research purposes, following institutional review board approval of Seoul National University Hospital and the informed consent of people undergoing in vitro fertilization (IVF) treatment. Seventy-three frozen-thawed pronuclear stage embryos produced by IVF were cultured to blastocyst stage in G1.2 and G2.2 media (Vitrolife AB, Göteborg, Sweden, http://www.vitrolife.com). Among them, 10 healthy blastocysts that showed clear ICM and trophectoderm under the microscope were selected for ICM isolation.

Isolation of ICM

ICM was isolated from the blastocysts by either immunosurgery [22] or the whole-embryo culture [1] method, as described previously. In the isolation of ICM by immunosurgery, nine blastocysts containing relatively large ICM were first treated with pronase (Sigma Chemical Corp., St. Louis, MO, http://www.sigma-aldrich.com) for about 4–5 minutes to dissolve the zona pellucida. Next, the outer trophectoderm layer was removed by the treatment of anti-human polyvalent immunoglobulins (Sigma) and guinea pig complement (Invitrogen, Carlsbad, CA, http://www.invitrogen.com). Isolated ICM was then plated onto mitomycin-C (Sigma)–treated STO (American Type Culture Collection [ATCC], Manassas, VA, http://www.atcc.org) feeder layers on gelatin-coated tissue culture plates in a 37°C incubator containing 5% CO_2. After 48 hours of plating, the culture medium was exchanged daily for half of the volume. Within 7–8 days of plating, clumps of the cells were isolated mechanically and replated on fresh feeder layers to derive SNUhES1 and 2.

To isolate ICM without risking cell loss, the whole-embryo culture method was used for a blastocyst containing small ICM, and the blastocyst was cultured on a mitomycin-C–treated STO feeder layer after digestion of zona pellucida with pronase. Within 7–8 days of plating, the central part of the cell clump (except the trophoblast) was isolated mechanically and subcultured on a fresh feeder layer to derive SNUhES3.

hESC Culture

hESCs were maintained on STO feeder layers in knockout Dulbecco's modified Eagle's medium (KO-DMEM) or DMEM/F12 (Invitrogen) supplemented with 20% knockout serum replacement (Invitrogen), 0.4 ng/ml basic fibroblast growth factor (bFGF; Invitrogen), 2 mM L-glutamine (Invitrogen), 1% nonessential amino acid (Invitrogen), 0.1 mM β-mercaptoethanol (Sigma), 50 U/ml penicillin, and 50 μg/ml streptomycin (PEST; Invitrogen). The culture medium was preincubated in a 37°C incubator 1 day before usage. The STO (mouse fibroblast) cell line was used as a feeder layer for the culture of undifferentiated hESCs [12]. The culture medium for expansion of the STO cells consisted of DMEM (high glucose with L-glutamine) (Invitrogen) supplemented with 10% fetal bovine serum (FBS; HyClone, Logan, UT, http://www.hyclone.com), 1 mM sodium pyruvate (Sigma), 1.5 g/L sodium bicarbonate

(Sigma), and PEST (Invitrogen). The expanded STO cells were treated with mitomycin-C and frozen. After thawing, these cells were seeded on 0.1% gelatin-coated culture dishes a day before the hESCs were plated.

Marker Analyses of hESCs

Marker analyses were performed at passages 8 to 10 for SNUhES1, passages 6 to 8 for SNUhES2, and passages 12 to 14 for SNUhES3. Markers were checked every 10 passages after that. An alkaline phosphatase (AP) diagnosis kit (Sigma) was used to detect AP activity. Briefly, the cells were washed with phosphate-buffered solution (PBS) twice, fixed with a citrate-acetone-formaldehyde solution for 1 minute, and then stained with AP staining solution for 15 minutes in the dark. Primary antibodies (Chemicon International, Temecula, CA, http://www.chemicon.com) were used at a dilution of 1:100 for detection of SSEA-1, SSEA-3, and SSEA-4. The primary antibodies were localized using biotinylated goat anti-mouse immunoglobulin G (IgG) as the secondary antibody, followed by treatment of a complex of avidin and horseradish peroxidase (Vectastain ABC system; Vector Laboratories, Burlingame, CA, http://www.vectorlabs.com). Finally, a peroxidase substrate kit DAB (Vector Laboratories) was used to localize the complex. hESC lines were karyotyped at passages 12 to 15 using the G-band method.

DNA Fingerprinting

DNA fingerprinting was performed as described previously [23]. Briefly, genomic DNA was extracted using the DNeasy tissue kit (Qiagen, Valencia, CA, http://www1.qiagen.com). DNA fingerprinting was performed on the three cell lines using the nine short tandem repeat (STR) loci—FGA, VWA, D3S1358, D18S51, D21S11, D8S1179, D7S820, D13S317, and D5S818—present in the AmpF/STR Profiler Plus PCR amplification kit (Applied Biosystems, Foster, CA, http://www.appliedbiosystems.com). For polymerase chain reaction (PCR), 2 ng of genomic DNA was amplified for 11 minutes at 95°C, followed by 28 cycles of 1 minute at 94°C, 1 minute at 59°C, 1 minute at 72°C, and a final extension for 45 minutes at 60°C. Aliquots of 1 μl of PCR product were mixed with 0.5 μl of GeneScan-500 ROX (Applied Biosystems) size standard and 2.5 μl of deionized formamide. The samples were then denatured at 95°C for 2–3 minutes and cooled in ice. Electrophoresis was carried out on a 4% polyacrylamide sequencing gel on an ABI 377 Genetic Analyzer (Applied Biosystems) for 2 hours. Fragment sizes were determined automatically using Genescan software version 2.1 and compared with the allelic ladder by Genotyper software version 2.1 (both from Applied Biosystems).

Expression Analyses of Oct-4, Cardiomyocyte Markers, and Telomerase

To monitor the expression levels of Oct-4 from undifferentiated cells and of cardiomyocyte markers from differentiated cells, total RNA from the cells was prepared using the RNeasy mini kit (Qiagen). cDNA was obtained using 1 μg of RNA with random hexamers and avian myeloblastosis virus (AMV) reverse transcriptase (RT; Invitrogen). PCR reactions were carried out with 5 μl of cDNA template, 10 pM of each primer, 8 μl of 2.5 mM dNTP mix, and 0.1 units of rTaq DNA polymerase (Takara Bio, Otsu, Shiga, Japan, http://www.takara-bio.co.jp/english/index.htm) in a volume of 50 μl. The following primer sets were used:

β-actin (forward: 5'-CGCACCCACTGGCATTGTCAT-3')
reverse: 5'-TTCTCCTTGATGTCACGCAC-3')
Oct-4 (forward: 5'-GGCGTTCTCTTTGGAAAGGTGTTC-3')
reverse: 5'-CTCGAACCACATCCTTCTCT-3')
GAPDH (forward: 5'-AGCCACATCGCTCAGACACC-3')
reverse: 5'-GTACTCAGCGGCCAGCATCG-3')
GATA4 (forward: 5'-AGACATCGCACTGACTGAGAA-3')
reverse: 5'-GACGGGTCACTATCTGTGCAAC-3')
Cardiac actin (forward: 5'-TCTATGAGGGCTACGCTTTG-3')
reverse: 5'-CCTGACTGGAAGGTTAGATGG-3')
ANF (forward: 5'-TAGGGACACACTGCAAGAGG-3')
reverse: 5'-CGAGGAAGTCACCATCAAACCAC-3')

Samples were amplified in a thermocycler under the following conditions for 32 cycles: first, the denaturing step at 95°C for 40 seconds, then the annealing step at 53°C–60°C for 40 seconds, and finally the amplification step at 72°C for 40 seconds. PCR products of Oct-4 and cardiomyocyte markers were normalized based on the β-actin or GAPDH signals. For detection of the cardiomyocyte marker *c*TnI by immunostaining, mouse anti-*c*TnI antibody (1:100; Chemicon) and Alexa Fluor 488 (green)–labeled donkey anti-mouse IgG (1:200; Molecular Probes, Eugene, OR, http://www.probes.com) were used as primary and secondary antibodies, respectively. Detection of telomerase activity was performed using the $TRAP_{EZE}$ Telomerase Detection Kit (Chemicon) according to manufacturer's instruction. hESC lines were analyzed at passages 15 to 20. Heat inactivation of samples was done at 85°C for 10 minutes. PCR products were analyzed on a 12.5% nondenaturing polyacrylamide gel and stained with SYBR green I (Sigma).

Teratoma Formation in Severe Combined Immunodeficient (SCID) Mice

Approximately 500 hESC colonies at approximately 20 passages were injected into the rear leg muscles of 4-week-old male SCID-beige mice (two mice per cell line). Eight weeks later, the resulting teratomas were examined histologically. All three cell lines produced teratomas.

Transmission Electron Microscopy

hESCs and embryoid bodies (EBs) were collected at different stages and fixed with 2.5% glutaraldehyde in 0.1 M phosphate buffer (pH 7.4) for 20 minutes at room temperature. After being rinsed for 10 minutes in the same buffer, the cells were post-fixed with 1% OsO_4 in 0.04 M phosphate buffer containing 0.14 M sucrose for 10 minutes at 4°C. Following dehydration with ethanol series and infiltration with epoxy resin, cells were transferred to beam capsules for polymerization in the oven. The capsules were separated from the polymerized resin with a razor blade, and embedded cells in hardened blocks were viewed with an optical microscope so that the appropriate area was chosen for ultrathin sectioning. Subsequently, ultrathin sections were obtained using an ultramicrotome (Sorvall MT-6000; DuPont, Wilmington, DE, http://www.dupont.com) with a diamond knife. Heavy metal staining was done with 4% uranyl acetate and lead citrate, and the samples were examined through the electron microscope (H-600; Hitachi, Tokyo, http://www.hitachi.com) at 50 kv.

In Vitro Differentiation into Cardiomyocytes

Differentiation into cardiomyocytes from hESCs was based on the method of Kehat et al. [3] with modifications. Briefly, undifferentiated hESC colonies were detached by treatment with collagenase IV (Invitrogen) for about 1 hour at 37°C. EBs were formed from suspension culture of hESC colonies in bacterial culture dishes and induced into mesodermal fate using DMEM/F12 medium (Invitrogen) supplemented with 20% knockout serum replacement (Invitrogen) for 1 month. The EBs were next attached onto 1% gelatin-coated culture dishes and differentiated into cardiomyocytes in KO-DMEM (Invitrogen) supplemented with 20% FBS (HyClone) for 20 days.

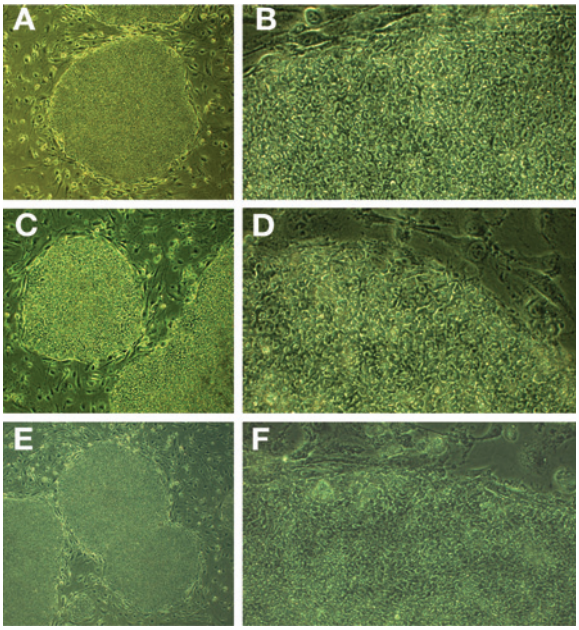

Figure 1. Derivation of human embryonic stem cell lines. Representative photographs of **(A, B)** SNUhES1, **(C, D)** SNUhES2, and **(E, F)** SNUhES3, respectively, are shown. SNUhES1 and 2 were derived from nine blastocysts using an immunosurgical method, while SNUhES3 was derived from a blastocyst using the whole-embryo culture method. Photographs were taken at low (×40; **A, C, E**) or high (×200; **B, D, F**) magnification.

Results

Derivation of Three hESC Lines: SNUhES1, SNUhES2, and SNUhES3

Blastocysts cultured from cryopreserved pronuclear stage embryos were used for establishment of hESC lines. Ten healthy blastocysts that showed both clear ICM and trophectoderm under the microscope were obtained from 73 embryos. The ICM was immunosurgically isolated from nine blastocysts containing a large ICM [22]. The remaining blastocyst had a relatively small ICM, and thus the ICM was separated by the whole-embryo culture method [1] to reduce the risk of cell loss. ICM isolated by both methods was plated onto fresh mouse STO feeder layers. After 5–7 days of culture, clumps of small, tightly packed cells proliferated from three (two of nine ICM isolated by immunosurgery and one isolated by whole-embryo culture) of the 10 ICM. These clumps were mechanically dissociated and replated onto fresh feeder layers. The replated cell clumps after several passages gave rise to flat colonies of cells with defined borders that morphologically resembled human or primate ESCs (Fig. 1A, C, and E). Under high magnification (×200), these cells showed a high ratio of nucleus to cytoplasm and prominent nucleoli (Fig. 1B, D, and F; Fig. 2A), as described previously. Each of SNUhES1, 2, and 3 cell lines was passaged for more than 90, 120, and 100 passages, respectively, while maintaining an undifferentiated state in the presence of the STO feeder layer. During routine passage of the cells, spontaneous differentiation was observed in some colonies even in the presence of the STO feeder layer. Differentiation usually happened in the central part of the colony or in its periphery, and the differentiated portions were manually removed before passaging undifferentiated cells.

Marker Expression, Karyotyping and DNA Fingerprinting of hESC Lines

Pluripotent hESCs have unique characteristics. In general, they show high expression levels of AP, SSEA-3, SSEA-4, TRA-1-60, TRA-1-81, Oct-4, and telomerase [10–13]. We began to investigate whether our hESC lines fit these criteria. As shown in Figure 3A, our cell lines showed a high level of AP activity. Elevated expression of this enzyme is associated with undifferentiated pluripotent stem cells [10, 11]. Immunophenotyping of the hESCs was performed using a series

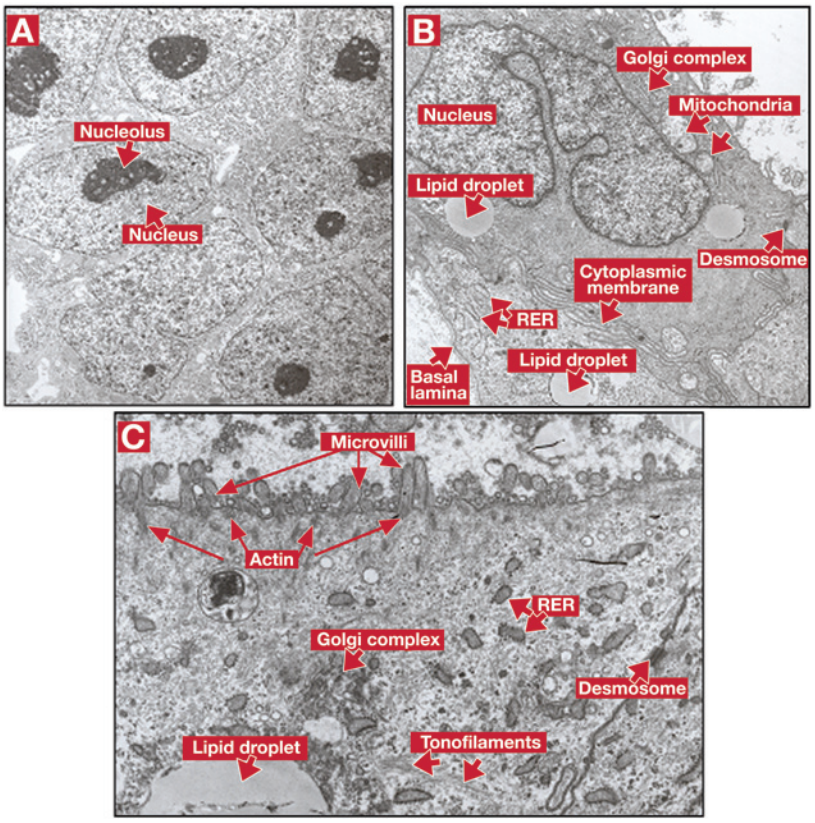

Figure 2. Fine structures of undifferentiated and differentiated hESCs. Morphological comparison between **(A)** undifferentiated and **(B, C)** differentiated hESCs analyzed by electron microscopy. The two types of cells clearly showed a big morphological difference. Undifferentiated hESCs have large nuclei with prominent nucleoli, whereas differentiated hESCs exhibit mature cellular organelles. Magnification: **A**, ×3.5K; **B**, ×8.0K; **C**, ×12K. Abbreviations: hESC, human embryonic stem cell; RER, rough endoplasmic reticulum.

of antibodies that detect cell surface markers. Our hESCs stained positively for SSEA-3, SSEA-4, TRA-1-60, and TRA-1-81 (Fig. 3C–F) but not SSEA-1 (Fig. 3B), a marker for mESCs. Staining intensity for SSEA-4 was consistently strong, but the intensity for SSEA-3 was relatively weak and variable among colonies, as reported previously [10]. SSEA-3 and SSEA-4 are glycoproteins specifically expressed in early embryonic development and by undifferentiated hESCs [10, 11]. TRA-1-60 and -81 are tumor-related antigens that are normally synthesized by undifferentiated hESCs [10, 11]. In addition, Oct-4 expression was observed only in undifferentiated hESCs, and its expression disappeared when hESCs differentiated (Fig. 4A). Oct-4 is a transcription factor that is essential for establishment and maintenance of undifferentiated hESCs and mESCs [11, 12, 24].

High levels of telomerase activity, a useful marker for identifying undifferentiated hESCs [10], were also observed in the three cell lines (Fig. 4B). Undifferentiated SNUhES1 (lane 4), 2 (lane 6), and 3 (lane 8) showed the same high activity as the positive control (lane 1) provided by the kit, but heat-inactivated samples (lanes 2, 5, 7, 9, and 11) and the STO feeder layer (lane 10) did not retain any telomerase activity. The high level of telomerase activity in these cell lines indicates that they have a potential to infinitely proliferate [10]. Thus, from this pattern of marker expression, these cell lines satisfy the criteria that characterize existing, pluripotent hESCs. Karyotyping was performed at passages 12 to 15, and all three cell lines retained

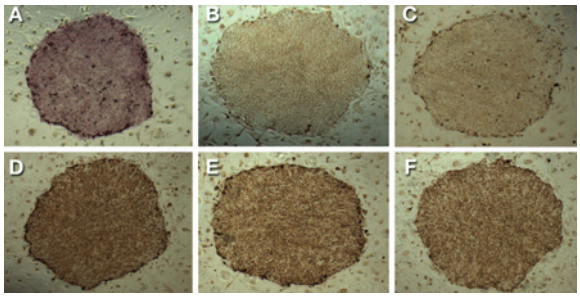

Figure 3. Marker analyses of hESCs. Staining of ESC markers such as **(A)** alkaline phosphatase, **(B)** SSEA-1, **(C)** SSEA-3, **(D)** SSEA-4, **(E)** TRA-1-60, and **(F)** TRA-1-81 are shown in SNUhES3 cells (×150 magnification). Similar results were obtained for the cell lines SNUhES1 and 2. Abbreviation: hESCs, human embryonic stem cells.

normal karyotypes (Fig. 5). In this assay, SNUhES1 and SNUhES3 had 46,XY karyotypes (Fig. 5A and C), whereas SNUhES2 showed a 46,XX karyotype (Fig. 5B). DNA fingerprinting was performed for these cell lines (Table 1). From the study of the nine STR loci [25], it is clear that these three cell lines were derived from different embryos. These fingerprinting results also provide useful information for identification of each cell line after cell distribution.

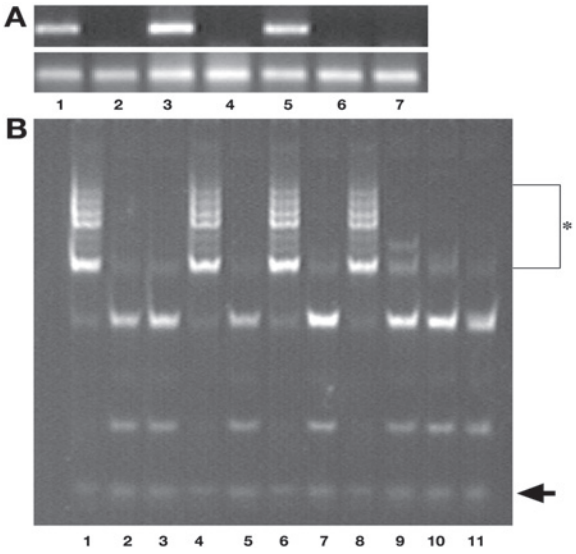

Figure 4. Expression of Oct-4 and telomerase in hESC lines. **(A):** Oct-4 expression in hESC lines: lane 1, undifferentiated SNUhES1; lane 2, differentiated SNUhES1; lane 3, undifferentiated SNUhES2; lane 4, differentiated SNUhES2; lane 5, undifferentiated SNUhES3; lane 6, differentiated SNUhES3; lane 7, STO feeder layer. **(B):** SNUhES cell lines express high levels of telomerase activity. A 36-bp internal control was used for amplification efficiency and quantification, as indicated by the arrow. A ladder of telomerase products amplified by PCR is shown with six base increments starting at 50 nucleotides at the portion indicated by the asterisk. Lane 1, positive control provided by kit; lane 2, heat-inactivated positive control; lane 3, PCR control without addition of template; lane 4, undifferentiated SNUhES1; lane 5, heat-inactivated SNUhES1; lane 6, undifferentiated SNUhES2; lane 7, heat-inactivated SNUhES2; lane 8, undifferentiated SNUhES3; lane 9, heat-inactivated SNUhES3; lane 10, STO feeder layer; lane 11, heat-inactivated STO feeder layer. Abbreviations: hESC, human embryonic stem cell; PCR, polymerase chain reaction.

Differentiation Potentials of hESCs in SCID Mice

An important property of ESCs is their ability to differentiate into all kinds of somatic cell types. To test this potential in vivo, the hESCs were injected into SCID mice [10–13]. As shown in Figure 6, these cells produced teratomas in each injected SCID mouse. Teratomas were found to contain tissues of the three embryonic germ layers: endoderm (gut-like structure [Fig. 6A] and gut epithelium [Fig. 6B]), mesoderm (cartilage [Fig. 6C]), and ectoderm (neural rosettes [Fig. 6D]). When these cell lines were cultured in a feeder-free condition, differentiation occurred rapidly in vitro (data not shown). When cultured on bacterial Petri dishes, these cell lines also showed a potential to make EBs, intermediates during the process of differentiation. Thus, these results suggest that the established cell lines are pluripotent even after prolonged proliferation.

Structural Differences between Undifferentiated and Differentiated hESCs

It was reported that undifferentiated hESCs have a high ratio of nucleus to cytoplasm [10]. This fact prompted us to investigate the structural differences between undifferentiated and differentiated hESCs in more detail using EM. Expanded undifferentiated colonies and EBs (8 weeks old) were used for analyses by transmission EM (TEM). As expected [10], the nucleus to cytoplasm ratio was high in undifferentiated hESCs (Fig. 2A). In addition, several other features were observed in these cells: They had indistinct cell membranes, free ribosomes, and ovoid nuclei with one to three reticulated nucleoli. Among the cellular organelles, small mitochondria with a few crista, a characteristic of premature cells, were occasionally found, but others such as rough endoplasmic reticulum (RER), Golgi complex, and lipid droplet were not observed. In contrast, differentiated cells showed highly developed cellular organelles such as extensive Golgi complexes associated with small secretory vesicles and ER studded with ribosomes (Fig. 2B, C), indicating that cells are actively synthesizing secretory

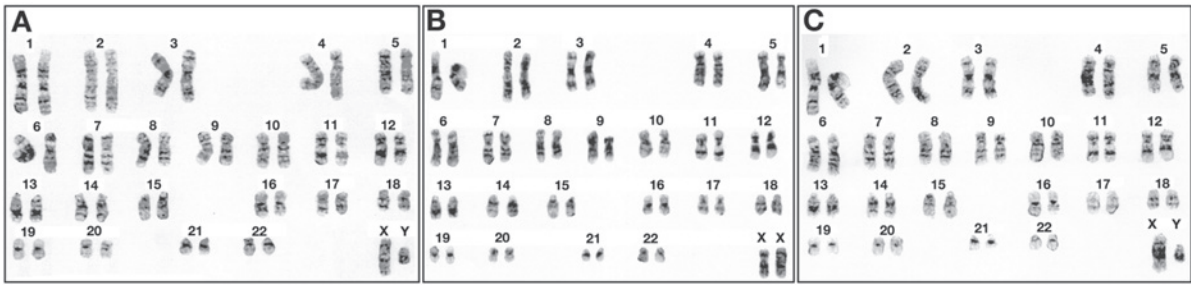

Figure 5. Karyotypes of SNUhES cell lines. When analyzed by G-staining method, karyotypes of after 12–15 passages were found to be normal: **(A)** SNUhES1, 46,XY, **(B)** SNUhES2, 46,XX, and **(C)** SNUhES3, 46,XY.

proteins as in somatic tissues. Organelles like lipid droplet and large mitochondria were also evident. Cytoplasmic membranes were irregular and extensively developed to enlarge the interface between cells. The existence of desmosomes and tonofilaments suggests that these cells differentiated into epithelial cells. Microvilli (shown in Fig. 2C) are similar (e.g., columnar and dense) to those of gastric epithelial cells. Cytoskeleton components such as actin and tonofilaments were also shown. Taken together, these results clearly show that undifferentiated hESCs have a relatively simple structure during proliferation, whereas the differentiated cells resemble epithelial cells and display all kinds of cellular organelles for intracellular and intercellular activities such as protein transport, as shown in adult somatic cells.

Table 1. DNA fingerprinting for SNUhES cell lines: distribution of alleles for the nine short tandem repeat loci in the three human embryonic stem cell lines

Allele	SNUhES1	SNUhES2	SNUhES3
D3S1358	17–16	17–16	16–16
D5S818	11–10	12–11	10–09
D7S820	11–11	10–08	12–11
D8S1179	14–10	16–12	15–14
D13S317	12–10	11–10	10–09
D18S51	16–14	17–13	13–12
D21S11	33.3–31	31–30	31.3–31.3
VWA	18–17	17–17	19–16
FGA	22–21	23–21	25–23
Gender	XY	XX	XY

Numbers indicate the genotype of alleles.

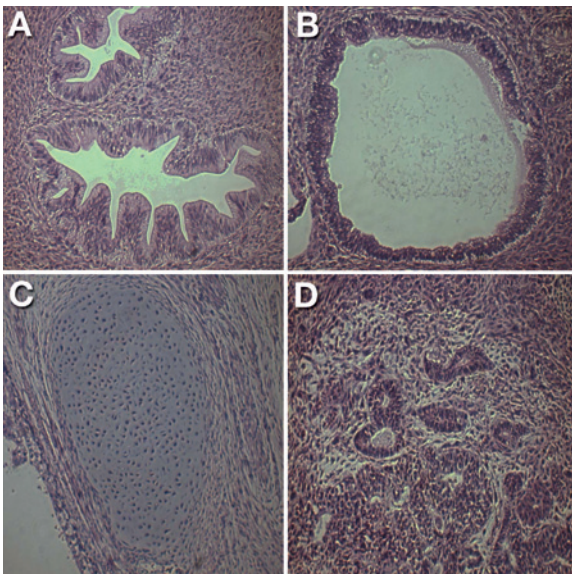

Figure 6. Teratoma formation after injection of human embryonic stem cells into severe combined immunodeficient mice. The tissues were stained with hematoxylin and eosin. **(A):** Gut-like structure (endoderm) from SNUhES1. **(B):** Gut epithelium-like tissue (endoderm) from SNUhES2. **(C):** Cartilage-like tissue (mesoderm) from SNUhES3. **(D):** Neural rosettes-like structure (ectoderm) from SNUhES1.

In Vitro Differentiation into Cardiomyocytes

To examine the differentiation potentials of three cell lines into cardiomyocytes, EBs formed from hESC colonies were first induced into mesodermal fate in a suspension culture and then differentiated into cardiomyocytes after attachment onto culture dishes. In general, mesodermal markers (e.g., enolase, cartilage matrix protein) began to be expressed approximately 18 days after suspension culture of EBs in all three cell lines. Thus, based on the expression of mesodermal markers, we attached 20-, 25-, and 30-day-old EBs onto gelatin-coated culture dishes after suspension culture. After further differentiation (~20 days) of attached EBs, contracting clusters were found from 30-day-old EBs but not from 20- or 25-day-old EBs. Contracting EBs were made from SNUhES3 most efficiently (~20% of total clusters), but they were seldom found in SNUhES1 and 2. These contractions continued for up to 4 weeks.

Using immunocytochemistry, the presence of cTnI, a cardiac-specific protein that is involved in the regulation of cardiac muscle contraction [26], was studied in differentiated EBs. As shown in Figure 7A–C, all three SNUhES cell lines expressed cTnI. However, among three cell lines, SNUhES1 and 3 showed a relatively strong expression of cTnI in comparison with SNUhES2, which revealed a weak expression of cTnI. SNUhES1, 2, and 3 cells gave rise to about 40%, 19%, and 60%, respectively, in the number of cTnI-positive cells among 4,6-diamidino-2-phenylindole–positive total cells (data not shown). These results indicate that of the three cell lines, SNUhES3 differentiates into cardiomyocytes most effectively.

Several other cardiac markers were analyzed from the SNUhES3 by RT-PCR. Figure 7D shows that GATA4, ANF, and cardiac actin (cACT) were also more highly expressed in cells differentiated from SNUhES3 (lane 2) than in undifferentiated cells (lane 1). GATA4 is known to be expressed in precardiac mesoderm of the developing heart [27], and ANF is a hormone that is expressed in ventricular cardiomyocytes [28].

Discussion

To establish hESC lines, we used 73 cryopreserved embryos produced by IVF. These embryos were cultured to blastocyst stage for 5–7 days. A blastocyst showing clear ICM and trophectoderm under the microscope was judged as a healthy blastocyst. In total, 10 healthy blastocysts were

developed from 73 embryos. Among them, nine blastocysts showed a relatively large ICM and one contained a small ICM. We separated the ICM from nine blastocysts using immunosurgery, resulting in the derivation of SNUhES1 and 2 cell lines. In contrast, we used whole-embryo culture method for the small ICM–containing blastocyst to reduce the risk of cell loss. The latter procedure resulted in the establishment of SNUhES3 from the blastocyst. Thus, the derivation method depended on the size of the ICM in the healthy blastocysts. We also obtained seven unhealthy blastocysts from the same 73 embryos that contained indistinguishable ICM and trophectoderm. To isolate ICM from the unhealthy blastocysts, the whole-embryo culture method was used, but it was impossible to establish hESC lines after 7-day culture because only the trophectoderm was expanded. Therefore, for successful establishment of hESC lines, it is important to first get healthy blastocysts from embryos, and then a method between immunosurgery and whole-embryo culture should be selected, depending on the size of the ICM.

The hESC lines that we derived here are similar in properties to those described by several groups [10–13]. They showed a similar morphology to already established hESCs (Fig. 1) and expressed surface markers of hESCs, including SSEA-3, SSEA-4, TRA-1-60, and TRA-1-81 but not an mESC marker, SSEA-1 (Fig. 3B–F). These cells also expressed high levels of AP activity (Fig. 3A) and Oct-4 (Fig. 4A) that are markers for both hESCs and mESCs. Oct-4 is a transcription factor that is limited to pluripotential cell populations, and its expression is downregulated during differentiation. As shown in Figure 4A, Oct-4 expression was extinct in a differentiated state. In addition, these cell lines showed high levels of telomerase activity (Fig. 4B), indicating that they can infinitely proliferate. Teratomas formed in SCID mice after injection of these hESCs included various cell types of the three embryonic germ layers (Fig. 6). Also, our hESC lines formed EBs in suspension culture on the bacterial culture dishes and retained a potential to differentiate into cardiomyocytes (Fig. 7). Taken together, our results suggest that our established hESC lines have the same properties as those reported in the existing hESC lines and a pluripotency to differentiate into all kinds of cells.

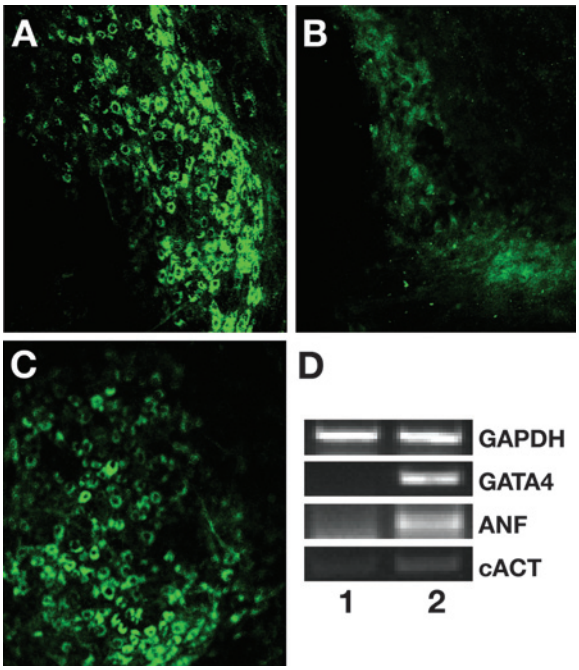

Figure 7. Analyses of embryonic stem cell–derived cardiomyocytes by immunostaining and reverse transcription polymerase chain reaction. **(A–C):** Immunostaining of differentiated EBs with mouse anti-cTnI antibody and Alexa Fluor 488 (green)–labeled donkey anti-mouse immunoglobulin G on SNUhES1, 2, and 3, respectively. **(D):** Expression of cardiac-specific markers in EBs (lane 2) differentiated from SNUhES3 compared with undifferentiated SNUhES3 (lane 1). Abbreviation: EB, embryoid body.

Our investigation using EM provides useful information regarding structural differences between undifferentiated and differentiated ESCs (Fig. 2). There have been reports that ESCs have a high ratio of nucleus to cytoplasm [10, 12]. Our EM analysis clearly shows unique characteristics in the undifferentiated hESCs compared with differentiated cells. Undifferentiated hESCs had large nuclei containing reticulated nucleoli, indistinct cell membranes, free ribosomes, and small mitochondria with a few crista, but not any other cellular organelles (Fig. 2A). In contrast, differentiated cells displayed highly developed cellular organelles such as Golgi complex, ER with ribosomes, lipid droplets, and large mitochondria (Fig. 2B, C). Observation of desmosomes and tonofilaments indicates that these cells differentiated into epithelial cells. The microvilli shown in Figure 2C are columnar and dense, suggesting that these cells differentiated into gastric epithelial cells. From these results, we can clearly see that undifferentiated ESCs have a unique, premature structure, whereas differentiated cells developed cellular machinery for various cellular activities, including protein secretion. The DNA fingerprinting for each cell line performed in this research provides information for cell line identity that could prove to be crucial in determining if contamination between cell lines occurred (Table 1).

From our observations and the reports from other groups [18–21], it is clear that all ESCs are different from each other in terms of differentiation potentials although they share characteristics in the undifferentiated state. For instance,

certain ESCs have a better ability than others in specific differentiation into neuronal phenotypes. Accordingly, the derivation of many hESCs and studies on them will provide more insights into the clinical application of hESCs. Further analysis of our cell lines in differentiation into other phenotypes will provide valuable information for application to cell replacement therapy.

Acknowledgments

We thank Dr. Jung Bin Lee (Forensic Medicine, College of Medicine, Seoul National University) for performing DNA fingerprinting. This research was supported by grant numbers SC11011 and SC12060 from the Stem Cell Research Center of the 21st Century Frontier Research Program funded by the Ministry of Science and Technology, Republic of Korea.

References

1 Evans MJ, Kaufman MH. Establishment in culture of pluripotential cells from mouse embryos. Nature 1981;292:154–156.

2 Martin GR. Isolation of a pluripotent cell line from early mouse embryos cultured in medium conditioned by teratocarcinoma stem cells. Proc Natl Acad Sci U S A 1981;78:7634–7638.

3 Kehat I, Kenyagin-Karsenti D, Snir M et al. Human embryonic stem cells can differentiate into myocytes with structural and functional properties of cardiomyocytes. J Clin Invest 2001;108:407–414.

4 Smith AG. Embryo-derived stem cells: of mice and men. Annu Rev Cell Dev Biol 2001;17:435–462.

5 Wichterle H, Lieberam I, Porter JA et al. Directed differentiation of embryonic stem cells into motor neurons. Cell 2002;110:385–397.

6 Brustle O, Jones KN, Learish RD et al. Embryonic stem cell-derived glial precursors: a source of myelinating transplants. Science 1999;285:754–756.

7 Lumelsky N, Blondel O, Laeng P et al. Differentiation of embryonic stem cells to insulin-secreting structures similar to pancreatic islets. Science 2001;292:1389–1394.

8 Bjorklund LM, Sanchez-Pernaute R, Chung S et al. Embryonic stem cells develop into functional dopaminergic neurons after transplantation in a Parkinson rat model. Proc Natl Acad Sci U S A 2002;99:2344–2349.

9 Bjorklund A, Lindvall O. Cell replacement therapies for central nervous system disorders. Nat Neurosci 2000;3:537–544.

10 Thomson JA, Itskovitz-Eldor J, Shapiro SS et al. Embryonic stem cell lines derived from human blastocysts. Science 1998;282:1145–1147.

11 Reubinoff BE, Pera MF, Fong CY et al. Embryonic stem cell lines from human blastocysts: somatic differentiation in vitro. Nat Biotechnol 2000;18:399–404.

12 Park JH, Kim SJ, Oh EJ et al. Establishment and maintenance of human embryonic stem cells on STO, a permanently growing cell line. Biol Reprod 2003;69:2007–2014.

13 Hwang WS, Ryu YJ, Park JH et al. Evidence of a pluripotent human embryonic stem cell derived from a cloned blastocyst. Science 2004;303:1669–1674.

14 Reubinoff BE, Itsykson P, Turetsky T et al. Neural progenitors from human embryonic stem cells. Nat Biotechnol 2001;19:1134–1140.

15 Zhang SC, Wernig M, Duncan ID et al. In vitro differentiation of transplantable neural precursors from human embryonic stem cells. Nat Biotechnol 2001;19:1129–1133.

16 Schuldiner M, Eiges R, Eden A et al. Induced neuronal differentiation of human embryonic stem cells. Brain Res 2001;913:201–205.

17 Assady S, Maor G, Amit M et al. Insulin production by human embryonic stem cells. Diabetes 2001;50:1691–1697.

18 Chung S, Sonntag KC, Andersson T et al. Genetic engineering of mouse embryonic stem cells by Nurr1 enhances differentiation and maturation into dopaminergic neurons. Eur J Neurosci 2002;16:1829–1838.

19 Kim JH, Auerbach JM, Rodriguez-Gomez JA et al. Dopamine neurons derived from embryonic stem cells function in an animal model of Parkinson's disease. Nature 2002;418:50–56.

20 Lee SH, Lumelsky N, Studer L et al. Efficient generation of midbrain and hindbrain neurons from mouse embryonic stem cells. Nat Biotechnol 2000;18:675–679.

21 Ward CM, Barrow KM, Stern PL. Significant variations in differentiation properties between independent mouse ES cell lines cultured under defined conditions. Exp Cell Res 2004;293:229–238.

22 Solter D, Knowles BB. Immunosurgery of mouse blastocyst. Proc Natl Acad Sci U S A 1975;72:5099–5102.

23 Gill P, Ivanov PL, Kimpton C et al. Identification of the remains of the Romanov family by DNA analysis. Nat Genet 1994;6:130–135.

24 Nichols J, Zevnik B, Anastassiadis K et al. Formation of pluripotent stem cells in the mammalian embryo depends on the POU transcription factor Oct4. Cell 1998;95:379–391.

25 Han GR, Lee YW, Lee HL et al. A Korean population study of the nine STR loci FGA, VWA, D3S1358, D18S51, D21S11, D8S1179, D7S820, D13S317 and D5S818. Int J Legal Med 2000;114:41–44.

26 Bhavsar PK, Brand NJ, Yacoub MH et al. Isolation and characterization of the human cardiac troponin I gene (*TNNI3*). Genomics 1996;35:11–23.

27 Stainier, D.Y. Zebrafish genetics and vertebrate heart formation. Nat Rev Genet 2001;2:39–48.

28 Zeller R, Bloch KD, Williams BS, et al. Localized expression of the atrial natriuretic factor gene during cardiac embryogenesis. Genes Dev 1987;1:693–698.